Spectrochimica Acta, Vol. 46B, No. 6/7, pp. 941–952, 1991
Printed in Great Britain.

0584-8547/91 $3.00 + .00
© 1991 Pergamon Press plc.

Influence of the practical resolution on limits of detection using high line number gratings in inductively coupled plasma atomic emission spectrometry*

J. M. MERMET† and M. CARRE
Laboratoire des Sciences Analytiques, Université Claude Bernard-Lyon I, 69622 Villeurbanne Cedex, France

and

A. FERNANDEZ‡ and M. MURILLO‡
Escuela de Quimica, Facultad de Ciencas, Universidad Central de Caracas, Caracas, Venezuela

(*Received* 15 *November* 1990; *accepted* 10 *December* 1990)

Abstract—The signal to background ratio and the relative standard deviation (RSD) of the background were studied in order to optimize the limits of detection in inductively coupled plasma atomic emission spectrometry. Czerny–Turner type monochromators equipped with high line number gratings (2400 and 3600 line mm^{-1}) working in the first and second orders were used. Because of the high incident and diffraction angles, leading to a magnification factor different from one, the influence of the slit width adjustment was studied. Symmetrical and asymmetrical slit widths were considered. It is shown that high signal to background ratios were obtained with slit widths of 10 μm. A degradation of the RSD of the background was observed for the narrow slit widths. This was not due to the dark current noise of the photomultiplier tube but rather to the limited number of photons. A longer integration time could alleviate this limitation. This was illustrated for the Cd I 228 nm line, which is one of the narrowest observed in this radiation source.

1. INTRODUCTION

ONE SIGNIFICANT feature of the inductively coupled plasma (ICP) used as a radiation source in atomic emission spectrometry (AES) is the high background resulting mainly from radiative recombination [1]. This background is significant above 200 nm and exhibits fluctuations which are the practical limitation in the detection of limits of detection. One way to express the limit of detection, c_L, has been extensively described by BOUMANS [2]:

$$c_L = k\, c\, RSD_B/SBR \tag{1}$$

where c is the concentration, RSD_B the relative standard deviation of the background B, and SBR the signal to background ratio. This relationship shows that an improvement in the value of c_L can be obtained by increasing the SBR if, at the same time, no degradation of the RSD_B is observed. In two papers, BOUMANS and VRAKKING [3] and BOUMANS [4] have described the significant role of the SBR in the calculation of c_L, in particular for the meaningful comparison of sets of values obtained for different dispersive systems. The results [3] allowed an unambiguous assessment of the limits of detection as a function of the frequency of the ICP generator, irrespective of the spectral bandpass of the dispersive system.

It has been shown [5, 6] that the SBR is inversely proportional to the experimental line width $\Delta\lambda_{exp}$. The experimental line width can be expressed as a quadratic function:

* This article was published in the Special Boumans Festschrift Issue of *Spectrochimica Acta*.

† Author to whom correspondence should be sent.

‡ Work performed while on leave from the University of Caracas.

Part of this work was presented at the meeting on Optical Spectroscopic Instrumentation and Techniques for the 1990s: Application in Astronomy, Chemistry and Physics, Las Cruces, New Mexico, U.S.A., 4–6 June 1990.

$$\Delta\lambda exp = (\Delta\lambda_L^2 + \Delta\lambda_o^2 + \Delta\lambda_S^2 + \Delta\lambda_Z^2)^{\frac{1}{2}} \quad (2)$$

where $\Delta\lambda_L$ is the physical line width, $\Delta\lambda_o$ is the theoretical resolution, $\Delta\lambda_S$ is the resultant spectral slit width (RSSW) and $\Delta\lambda_Z$ is the term due to optical aberrations and the inadequacy of the convolution, as the assumption of a quadratic function is only true for Gaussian, triangular and trapezoidal profiles.

At a given wavelength, the last three terms of Eqn (2) are constant and are equivalent to the instrumental profile or practical resolution $\Delta\lambda_{ins}$. The experimental line width is therefore equal to:

$$\Delta\lambda_{exp} = (\Delta\lambda_L^2 + \Delta\lambda_{ins}^2)^{\frac{1}{2}}. \quad (3)$$

Assuming a Gaussian shape of the line profile and a constant distribution of the background, a theoretical SBR can be calculated as a function of $\Delta\lambda_{ins}$. For instance, when $\Delta\lambda_{ins} = \Delta\lambda_L$, 68.2% of the area under the line profile is observed. When $\Delta\lambda_{ins} = 0.1\ \Delta\lambda_L$, only 8% of the area is observed, but the contribution of the background is divided by 10, so that the SBR is improved by 1.17. The relative variation of the SBR can be normalized as a function of the $\Delta\lambda_{ins}/\Delta\lambda_L$ ratio and is given in Fig. 1. It

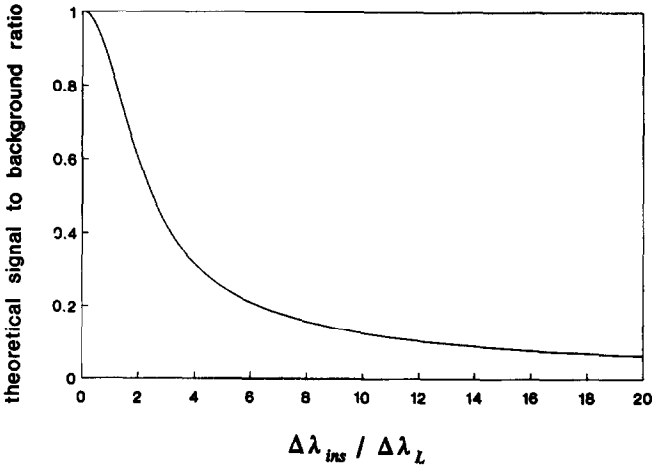

Fig. 1. Theoretical signal to background ratio normalized to one as a function of the instrumental profile to the physical line width ratio.

can be deduced that the SBR is almost constant when $\Delta\lambda_{ins}$ is less than 0.7 $\Delta\lambda_L$, is inversely proportional to the square of $\Delta\lambda_{ins}$ when $\Delta\lambda_{ins}$ is between 0.7 $\Delta\lambda_L$ and 2 $\Delta\lambda_L$, and is inversely proportional to $\Delta\lambda_{ins}$ when $\Delta\lambda_{ins}$ is greater than 2 $\Delta\lambda_L$. These conclusions are similar to those obtained empirically by BOUMANS and VRAKKING [3]. Their corresponding limits were $\Delta\lambda_L$ and 2 $\Delta\lambda_L$ for a variation of the SBR as a function of $\Delta\lambda_{exp}$. The values of the physical line widths $\Delta\lambda_L$ observed in ICP–AES has been reported for many lines [7] and are in the range of 0.9–7 pm when the Doppler effect is the main cause of line broadening. The best SBR values would be obtained for $\Delta\lambda_{ins}$ less than 1 pm for the narrowest lines. Several optical systems have been proposed to obtain a small instrumental profile:

(i) use of an echelle grating spectrometer [8,9];
(ii) use of a high resolution Fourier transform spectrometer [10];
(iii) use of a spectrometer equipped with a high line number grating working in the second order [5].

With an echelle grating spectrometer, it is possible to obtain an instrumental profile of less than 2 pm, depending on the order [3]. A practical limitation is the low throughput with narrow slit widths and the difficulty of obtaining an acceptable throughput below 200 nm. A Fourier transform spectrometer exhibits an unsurpassable resolution, but has not gained acceptance for analytical applications due to its limited dynamic range. Most commercial ICP systems based on a sequential spectrometer make use of an inteferometric grating with a line number of at least 1800 line mm^{-1}. Best experimental instrumental profiles measured at 230 nm [11] are in the range of 3 to 5 pm and are obtained in the second order with 2400 or 3600 line mm^{-1} gratings. The two main limitations in obtaining low instrumental widths are the resultant spectral slit width and the aberrations.

In this work, we will describe the consequences of using high line number plane gratings in the first and second order in order to observe values of $\Delta\lambda_{ins}$ less than 5 pm, and consequently high SBRs. In particular, we will deal with the parameters influencing the resultant spectral slit width and their influence on the RSD_B.

2. Theoretical Considerations

The resultant slit width is defined as the width of the exit slit or the image of the entrance slit, whichever is the greater. The RSSW is the product of the resultant slit width and the reciprocal linear dispersion (RLD). The RLD is given by:

$$RLD = \cos\beta/k\,n\,f, \tag{4}$$

where β is the diffraction angle, k the order, n the line number per mm, and f the focal length. Improvement in the RLD could be obtained by increasing the focal length of the monochromator. Practically, for thermal stability and aperture reasons, a focal length of 1 m is the greatest value used in commercial systems. An alternative for improving the RLD within the same optical system is therefore to increase the number of lines (2400 or 3600 line mm^{-1}) and to work in the second order [5]. The only limitation is the maximum upper wavelength which can be used, because of the angle limit (β or α equal to 90°). The upper wavelength is 270 nm and 410 nm for the 3600 line mm^{-1} and 2400 line mm^{-1} gratings, respectively.

In a plane grating monochromator, the difference $2i$ between the diffracted angle β and the incident angle α is a constant. It depends on the focal length, the distance between the entrance and exit slits, and the location of the grating [5]. The work presented here is based on the use of two 1-m Czerny–Turner type monochromators from Jobin–Yvon. They are utilized in the JY 38 and JY 38 Plus Jobin–Yvon ICP systems. The value of $2i$ is 14.74° and −13.42° for the 38 and 38 Plus monochromators, respectively. In the former optical system, the grating is oriented towards the entrance slit, in the latter, the grating is oriented towards the exit slit. From the grating formula and the value of $2i$, it is possible to calculate the value of β:

$$\beta = \arcsin(k\,n\,\lambda/2\cos i) \pm i. \tag{5}$$

The sign is "+" when the grating is oriented towards the entrance slit. As mentioned above, it is necessary to know whether the image of the entrance slit is greater than the exit slit in order to define the resultant slit width. As the focal lengths of the collimating and the camera mirrors are the same in each monochromator then, assuming no optical aberrations, the magnification factor G of the image of the entrance slit is:

$$G = \cos\alpha/\cos\beta. \tag{6}$$

For the 38 monochromator, β is greater than α, whereas with the 38 Plus monochromator α is greater than β. When the 38 monochromator made use of a 1200 line mm^{-1} grating, it can be seen from Table 1 that both α and β angles were less than 25° for $\lambda < 500$ nm. The correspondong magnification factor G was therefore

Table 1. Incident angle α, diffraction angle β, RLD (nm mm^{-1}) and magnification factor G of the entrance slit for a 1-m monochromator (JY 38) equipped with a 1200 or a 3600 line mm^{-1} plane grating

n	λ	α	β	RLD	G
1200	200	−0.22	14.12	0.808	1.03
	300	3.28	17.62	0.794	1.05
	400	6.83	21.17	0.777	1.06
	500	10.43	24.77	0.757	1.07
3600	200	14.10	28.44	0.244	1.10
	300	25.80	40.14	0.212	1.18
	400	39.35	53.69	0.164	1.31
	500	57.93	72.28	0.085	1.74

always less than 1.08, which indicates that for two slits of the same width, the image of the entrance slit was similar to the exit slit. As mentioned above, however, it is necessary to use a high line number grating to improve the RLD. When a 3600 line mm^{-1} grating is used in the same monochromator (Table 1), larger angles are obtained, corresponding to a value of G of up to 1.8. Moreover, this magnification increases with increasing wavelength. The greatest value of G is obtained when the wavelength tends to the upper limit ($\beta = 90°$, i.e. $\lambda = 540$ nm). For symmetrical slit widths, the RSSW is dependent on the entrance slit width.

Different conclusions are obtained for the 38 Plus monochromator configuration, as the magnification factor is less than one (Table 2). For symmetrical slit widths therefore,

Table 2. Incident angle α, diffraction angle β, RLD (nm mm^{-1}) and magnification factor G of the entrance slit for a 1-m monochromator (JY 38 Plus) equipped with a 2400 line mm^{-1} grating working in two k orders

k	λ	α	β	RLD	G
1	200	20.69	7.27	0.413	0.94
	300	27.96	14.54	0.403	0.91
	400	35.61	22.19	0.386	0.88
	500	43.88	30.46	0.359	0.84
2	200	35.61	22.19	0.193	0.88
	300	53.17	39.75	0.160	0.78
	400	81.86	68.44	0.076	0.38

the RSSW is dependent on the exit slit width. With both configurations, the factor G is the same for a given wavelength λ in the 1st order and for λ/2 in the 2nd order.

For a 2400 or a 3600 line mm^{-1} grating working in the second order, the upper wavelength limit is readily reached (410 and 270 nm, respectively) as many analytical lines are in this wavelength range. Working near these wavelength limits, the magnification factor G will differ from one and will vary with the wavelength.

For symmetrical slit width adjustment, the variation of the RSSW as a function of the wavelength will depend on the optical mount. The RLD always decreases with the wavelength. For $\beta > \alpha$, the resultant slit width is equal to the image of the entrance slit and increases with wavelength. For $\alpha > \beta$, the resultant slit width is equal to the exit slit and is independent of wavelength. Actually, the RSSW is always improved as a function of the wavelength irrespective of the orientation of the grating (Table 3).

Table 3. Resultant slit widths (RSW, μm) for the two 38 and 38 Plus 1-m monochromators with symmetrical (20 μm) slit widths and corresponding resultant spectral slit width ($\Delta\lambda_S$, nm mm^{-1}) in the first order

	JY38 (n=3600)		JY 38 Plus (n=2400)	
λ	RSW	$\Delta\lambda_S$	RSW	$\Delta\lambda_S$
200	22	0.54	20	0.83
300	24	0.50	20	0.81
400	26	0.43	20	0.77
500	35	0.30	20	0.72

3. Results

3.1. *Role of the slit width adjustment on the experimental line width*

To illustrate the role of the slit widths, several experiments were performed with the 38 monochromator. Two test lines were selected: Cd I 228.8 nm and Ba II 455.5 nm as their physical line width are well documented (1.5 and 3.5 pm [7], respectively). Also, Ba II 455.5 nm is close to the upper wavelength limit of the 3600 line mm^{-1} grating working in the first order. As the Ba line wavelength is almost double the Cd one, this allows a comparison between the first and second orders. At 455 nm, the RLD (first order) is 0.126 nm mm^{-1} and the magnification G is 1.47, whereas at 228 nm (first order), the values are 0.236 nm mm^{-1} and 1.12, respectively.

Several combinations of slit widths were used at 455 nm. We will describe results obtained with the following combinations: (i) 20 μm fixed entrance slit and variable exit slit (10–100 μm); (ii) 35 μm fixed entrance slit and variable exit slit; (iii) variable entrance slit and 50 μm fixed exit slit. These combinations are summarized as 20/*, 35/*, and */50, respectively. Similarly at 228 nm, we will describe results obtained for a variable entrance slit and a 50 μm fixed exit slit (*/50). As explained above, at 455 nm, the value of $\Delta\lambda_s$ is constant up to an exit of 30 μm for the first set of slits, up to 50 μm for the second set and up to an entrance slit of 35 μm for the third set, because of the magnification value. Therefore, the 35/* and */50 combinations exhibit the same $\Delta\lambda_S$ up to 35 μm and the 20/* and 35/* ones from 50 μm. At 228 nm, the value of $\Delta\lambda_S$ is constant up to an entrance slit of 45 μm. To compare experimental line widths with RSSW values, theoretical values of $\Delta\lambda_S$ are plotted in Fig. 2 according to the various slit width combinations. The influence of wavelength on $\Delta\lambda_s$ can be seen for the */50 adjustment at 228 nm and 455 nm.

In Fig. 3, the effect of the variable slit width on the experimental line widths is given for the 38 monochromator. These values are compared with those obtained from relation (2). At a given wavelength, $\Delta\lambda_L$, $\Delta\lambda_O$ (equal to 0.5 pm) and $\Delta\lambda_Z$ are constant so that the experimental line widths can be expressed as:

$$\Delta\lambda_{exp} = (a + \Delta\lambda_S^2)^{\frac{1}{2}}. \quad (7)$$

Using Eqn (7), in the first part of the curve, a horizontal straight line is obtained as $\Delta\lambda_S$ and $\Delta\lambda_{exp}$ are constant with change in the variable slit width. In the second part of the curve, the RSSW varies linearly with the variable slit width and $\Delta\lambda_{exp}$ is equal to $\Delta\lambda_S$ for $\Delta\lambda_S \gg a$. Experimentally, the curve exhibits two asymptotes. Using these asymptotes, the calculated values of the aberration term at 455 and 228 nm are 1.3 and 4.8 pm, respectively. The only discrepancy (Fig. 3) between the experimental values and the theoretical ones from Eqn (7) is observed near the intersection of the two lines. This is probably because the aberration term is not correctly taken into

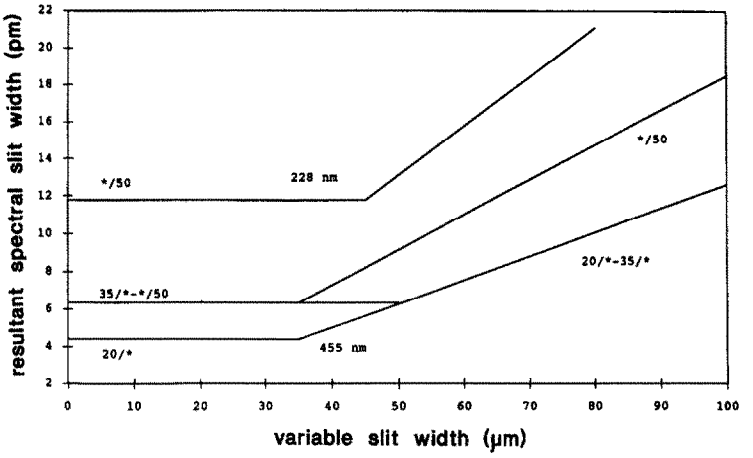

Fig. 2. Resultant spectral split width calculated for the JY 38 monochromator equipped with a 3600 line mm^{-1} grating as a function of the variable slit width. Various slit widths combinations were used. The term */50 indicates that a variable entrance slit width (*) and a fixed exit slit width of 50 μm were used (50). Calculation was carried out for Ba 455 nm line and Cd 228 nm line in the 1st order.

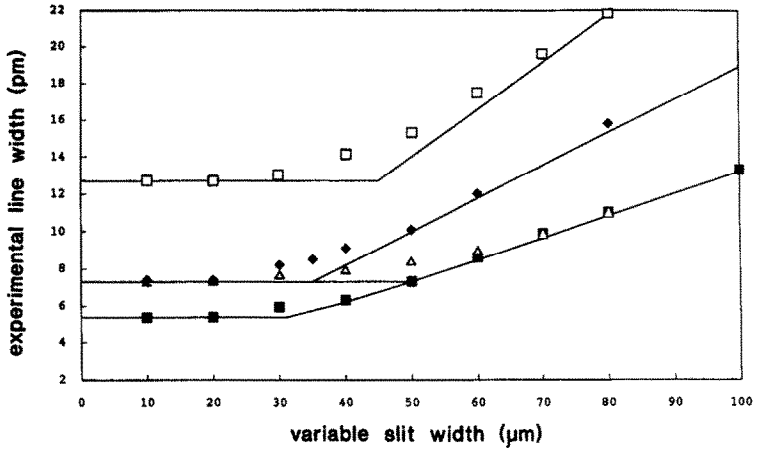

Fig. 3. Comparison of the experimental line widths and the values obtained using Eqn (2). Slit width combinations were the same as in Fig. 2.

account in relation (2) and not considered in relation (6). Nevertheless, the aberration term is drastically reduced when the wavelength increases.

A similar experiment was carried out for the 38 Plus monochromator. The Cd I 228 nm line was observed in the 2nd order with the 50/* slit width combinations (RLD = 0.34 nm mm^{-1}). Results are shown in Fig. 4. An aberration term of 6 pm was found to give the best fitting with the experimental values (Fig. 4). The agreement is not as good as in the previous experiment. The aberration term was not found to be constant along the two asymptotes and the value of 6 pm was only a compromise. The overall variation was between 4 and 7 pm. This can be due to a wrong calibration of the slit widths and, consequently, to an uncorrect calculation of the RSSW.

3.2. *Consequence of slit width adjustment*

A first consequence of a magnification factor different from one is that the results obtained with a slit adjustment of 20/35 μm will produce an experimental line width different (6.2 pm) from that obtained with a 35/20 μm adjustment (7.5 pm).

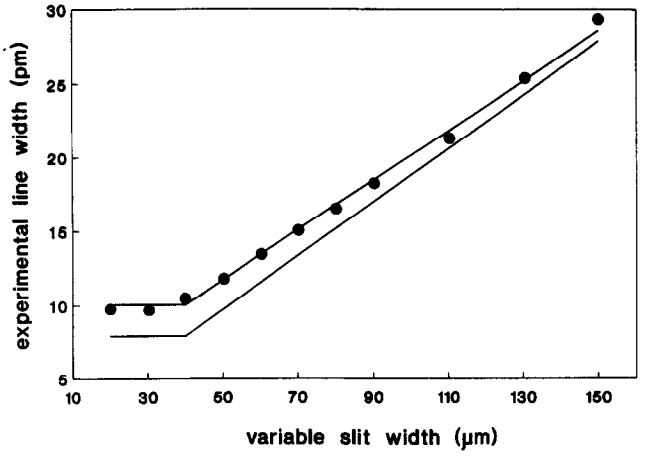

Fig. 4. Comparison of the resultant spectral slit width, the experimental line widths and the values obtained using Eqn (2) for the Cd 228 nm line. The monochromator was the JY 38 Plus equipped with a 2400 line mm^{-1} grating working in the second order. The slit width combination was 50/*. The upper curve is obtained using Eqn (2), the lower curve is the RSSW.

Moreover, the variation of either one slit or both slits has not the same consequence on the measured intensity of the background and the line. The throughput (photon flux) at the exit of a monochromator depends on the geometric etendue and the resultant spectral slit width. If an area of the source viewed by the monochromator has both the spectral distribution over the spectral bandpass and the spatial distribution constant over the area (unfeatured background), the throughput varies as follows:

(i) When only one slit width is modified so that the resultant slit width increases, the etendue is constant because it is limited by the narrower slit width. However, the throughput is proportional to the variable slit width.
(ii) When the two slit widths are adjusted, both the etendue and the resultant spectral slit width are proportional to the slit width. The throughput is therefore proportional to the square of the slit width.

A similar conclusion can be made if the resultant spectral slit width is smaller than the physical line width. In this instance, the top of the line is considered as a continuum.

Generally, with commercial ICP systems, the observation of a line corresponds to a physical line width which is smaller than the resultant spectral slit width. For a narrow line, a single slit width variation corresponds to a constant throughput. This is in contrast to the situation where both slits are varied corresponding to a throughput proportional to the slit width. An intermediate case can be described where the resultant slit width is of the same order as the physical line width, which can be the case in ICP–AES. An example is given for the Be I 234 nm line (experimental line width 4.7 pm) and the background at the same location using the 38 Plus monochromator equipped with a 2400 line mm^{-1} grating working in the second order (Figs 5 and 6). For a single slit variation (Fig. 6), a constant throughput is observed only when the physical line width is small compared with the RSSW.

3.3. *Studies of the experimental SBR*

As the instrumental profile $\Delta\lambda_{ins}$ is dependent on the slit width adjustment, we have carried out experiments using the Cd I 228.8 nm line. This line is one of the narrowest obtained from an ICP ($\Delta\lambda_L$ = 1.5 pm) and, therefore, should exhibit the lowest SBR with respect to the maximum value obtainable at a bandwidth equal to the physical line width. The 38 Plus monochromator equipped with a 2400 line mm^{-1} grating working in the second order was used in order to minimize the instrumental profile.

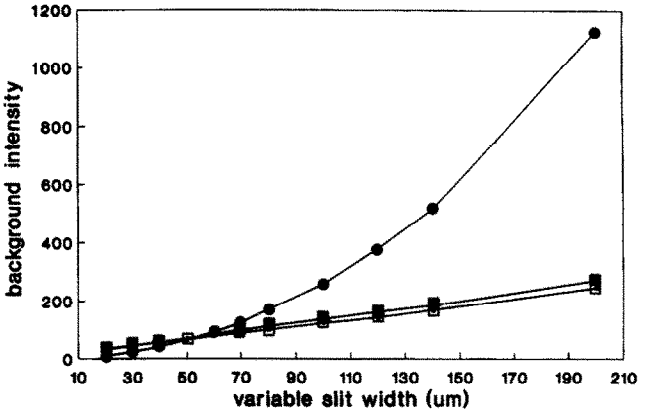

Fig. 5. Background intensity as a function of the variable slit width. (●) */* slit width combination; (⊡) 50/*; (■) */50.

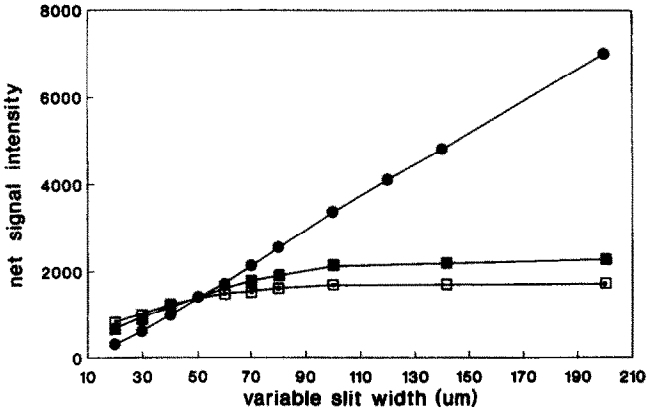

Fig. 6. Line intensity of Be 234 as a function of the variable slit width. (●) */* slit width combination; (⊡) 50/*; (■) */50.

The results are given in Fig. 7 for various slit width combinations (*/50, 50/*, and symmetrical adjustment */*). The results are superimposed (after normalization) on

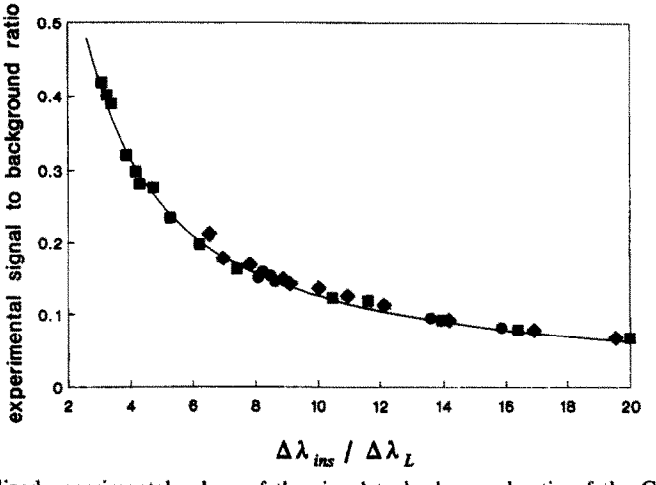

Fig. 7. Normalized experimental values of the signal to background ratio of the Cd 228 nm line for various slit width combinations: (■) */*; (♦) 50/*; (●) */50.

the theoretical curve given in Fig. 1. The agreement is good. The best measured instrumental profile was 4.7 pm (10/15 μm) which lead to a $\Delta\lambda_{ins}/\Delta\lambda_L$ ratio of 3. The corresponding value of the SBR was 40% of the maximum theoretical value. However, a higher SBR value was obtained for line widths greater than 4 pm. For instance, a value of 90% of the maximum was observed for Be I 234 nm (4.7 pm, i.e. a $\Delta\lambda_{ins}/\Delta\lambda_L$ ratio of 1) with the same dispersive system. At least for the largest line widths, the maximum SBRs can be obtained with a 2400 line mm^{-1} grating working in the second order. This grating was blazed by ion etching so that its efficiency was good in the second order. The 3600 line mm^{-1} grating used in the 38 monochromator was not optimized for the second order. However, its efficiency was still sufficient to perform experiments in this order. In this instance, the instrumental profile was 1.7 pm (10/10 μm), which lead to a $\Delta\lambda_{ins}/\Delta\lambda_L$ ratio of 1 for the Cd I 228 nm line and less than 1 for the Be 234 nm line. The use of such a grating blazed, for working in the second order, would provide SBRs equal or close to the maximum value. The only limitation would be the upper wavelength limit.

3.4. *The determination of limits of detection of cadmium and their dependence on the optical system used*

Using the average of 4 series of 10 replicates, values of the RSD_B were determined and used in relation (1) for $k = 3$, to calculate the limits of detection. Results are summarized in Fig. 8 for an integration time of 0.5 s per step using the same slit width

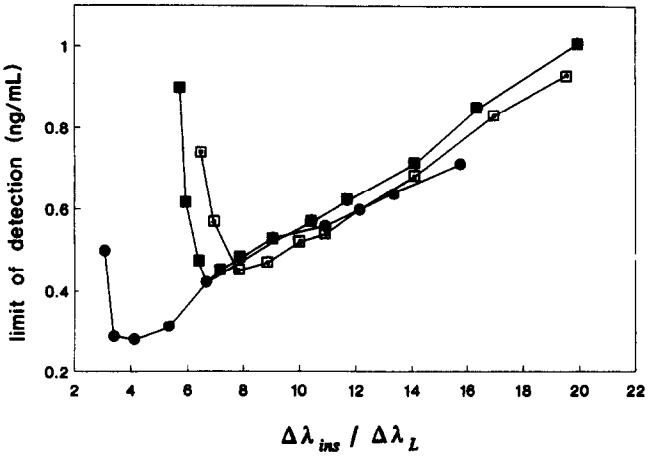

Fig. 8. Limits of detection of Cd as a function of the instrumental profile to the physical line width ratio for various slit width combinations: (●) */*; (▣) 50/*; (■) */50.

combinations as in Section 2.3. Clearly, the drastic change in the limit of detection must be attributed to the variation in RSD_B. The main causes of the background fluctuations [2] are the flicker noise due to the instabilities of the sample introduction system and the generator, the shot noise due to the random nature of the photon emission process, and the detector noise. Usually, the detector noise is considered as negligible when a photomultiplier tube (PMT) with a low dark current is used. For work with very narrow slits, it has been thought that the dark current fluctuations were a major contribution to the noise of the background. However, experiments (Table 4) carried out with a Hamamatsu R 166 UH solar blind PMT at 2 voltages (650 and 900 V) for slit widths equal to 10 μm showed that the contribution of the dark current noise was negligible against the fluctuations of the background. The use of a higher voltage (900 V) leads to a higher detection noise and a slight degradation of the limits of detection (Fig. 9). Therefore, it was more preferable to use 650 V and a

Table 4. Values of the dark current and its fluctuation in terms of standard deviation (SD) and relative standard deviation (RSD), and values of the background, its SD and RSD as a function of the slit widths (0.5 s integration time)

Slit width (μm)	PMT voltage (V)	Dark current (nA)	Offset (nA)	RSD (%)	SD (na)
closed	650	0.12	0.28	1	0.01
	900	2.3	0.28	6	0.14
		Background (nA)		RSD	SD
10/10	650	6.5		1.2	0.08
	900	60		2	1.2
20/20	650	19		0.6	0.1
	900	180		1	1.8
30/30	650	39		0.5	0.19
	900	450		0.6	2.8
40/40	650	68		0.5	0.3
	900	780		0.5	4.2

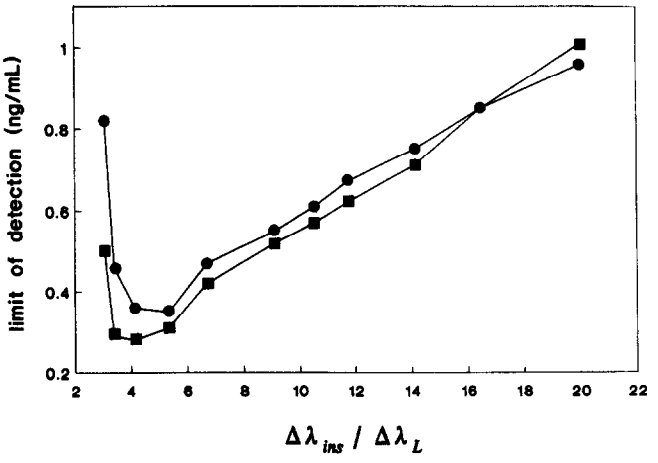

Fig. 9. Limits of detection as a function of the instrumental profile to the physical line width ratio for two voltages of the photomultiplier tube: (■) 650 V; (●) 900 V. The slit width combination was */*.

low noise amplifier at the output of the PMT. When using larger slit widths, the RSD_B decreased and tended to a lower limit of 0.3% at 650 V and 0.4% at 900 V. Clearly, the limitation for narrower slits is not directly linked to the dark current noise, but to the limited amount of photons observed during the integration time. This is illustrated in Fig. 10, where the RSD_B is measured as a function of the integration time per step for three slit width combinations: 10/10, 20/20 and 30/30. For the 10/10 slit widths, it is necessary to use an integration time of at least 2 s to obtain RSD_B less than 1%. This integration time is 0.5 s and 0.1 s for the 20/20 and 30/30 slit widths, respectively. The best limit of detection (0.17 ng ml^{-1}) was obtained for the 20/20 slit width combination and an integration time of 2 s. To obtain a similar limit of detection with the 10/10 slit width combination, an integration time longer than 10 s would be necessary. This could be a limiting factor as several steps are used for the peak search procedure. Drift may become a problem for long integration times.

When one of the slit widths decreases below the resultant slit width, the SBR is constant but the throughput varies with the width. The RSD_B is therefore degraded.

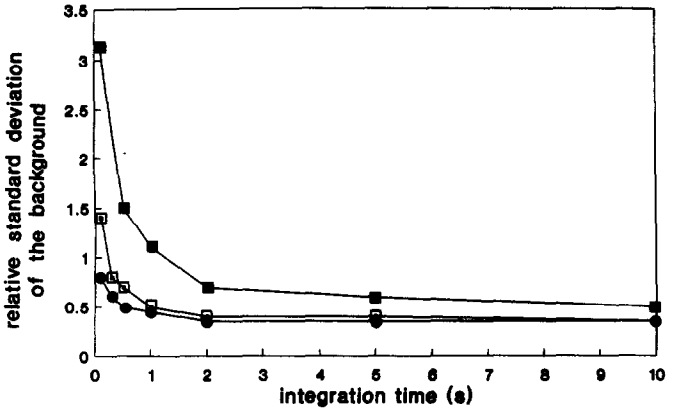

Fig. 10. Values of the RSD of the background as a function of the integration time for several slit width combinations: (■) 10/10; (⊡) 20/20; (●) 30/30.

A 10/20 slit width combination lead to a RSD_B of 1% whereas a 20/20 one lead to 0.7%. Consequently, the limit of detection is better for the latter combination.

3. Conclusions

It is possible to obtain the maximum SBR of the lines obtained from an ICP when the dispersive devices of commercial ICP systems are equipped with a high line number grating (>2400 line mm^{-1}) working in the second order, with adjustable slit widths down to 10 μm. It can be necessary to use long integration times to compensate for the limited number of photons with this configuration. This implies that no drift is observed during the peak search. It should be noted that the dark current noise is not a limitation in the value of the RSD_B.

Consequences of the use of such gratings are:

(i) a limited wavelength range because of the upper limit;
(ii) a drastic variation of the resultant spectral slit width due to the change in the reciprocal linear dispersion with wavelength;
(iii) the enhanced role of the entrance and the exit slits because the magnification factor is different from one.

Combination of a low background fluctuation with an ICP frequency greater than 27 MHz [3, 12, 13] and an SBR close to the maximum value therefore explains the excellent limits of detection obtained with this ICP system [12]. This work confirms that the SBR is an important parameter in the optimization of limits of detection and depends on the practical resolution of the optical system. However, RSD_B must be taken into consideration as its variation can be in the range of 0.35 to 3%, i.e. a factor of 10.

References

[1] A. Batal, J. Jarosz and J. M. Mermet, *Spectrochim. Acta* **36B**, 983 (1981).
[2] P. W. J. M. Boumans, *Basic Concepts and Characteristics of ICP-AES.* In: *Inductively Coupled Plasma Emission and Spectrometry,* Ed. P. W. J. M. Boumans, Part 1, Chap. 4, p. 100. Wiley, New York (1987).
[3] P. W. J. M. Boumans and J. J. A. M. Vrakking, *Spectrochim. Acta* **42B**, 553 (1987).
[4] P. W. J. M. Boumans, *Spectrochim. Acta* **44B**, 1325 (1989)
[5] J. W. McLaren and J. M. Mermet, *Spectrochim. Acta* **39B**, 1307 (1984).
[6] P. W. J. M. Boumans and J. J. A. M. Vrakking, *Spectrochim. Acta* **40B**, 1437 (1985).
[7] P. W. J. M. Boumans and J. J. A. M. Vrakking, *Spectrochim. Acta* **41B**, 1235 (1986).

[8] P. W. J. M. Boumans and J. J. A. M. Vrakking, *Spectrochim. Acta* **39B**, 1239 (1984).
[9] T. Hasegawa and H. Haraguchi, *Spectrochim. Acta* **40B**, 123 (1985).
[10] L. Faires, B. A. Palmer and J. W. Brault, *Spectrochim. Acta* **40B**, 135 (1985).
[11] J. M. Mermet, *J. Anal. Atom. Spectrom.* **2**, 681 (1987).
[12] B. Capelle, J. M. Mermet and J. Robin, *Appl. Spectrosc.* **36**, 102 (1982).
[13] M. Marichy, M. Mermet, M. Murillo, E. Poussel and J. M. Mermet, *J. Anal. Atom. Spectrom.* **4**, 209 (1989).